APPLICATION OF THE COMPONENT ELEMENT METHOD TO THE IMPACT DAMPED SIMPLE HARMONIC OSCILLATION

C.M. North
Rose-Hulman Institute of Technology
Box 145
5500 Wabash Avenue
Terre Haute, Indiana 47803
812-877-8216

and

R. E. Jones
Graduate Student
Texas A & M University
1917 Vinewood Drive
Bryan, Texas 77802
409-845-9599

ABSTRACT

Time histories of the impact damped simple harmonic oscillator in free decay are studied. The numerical technique of finite differences with central difference approximations is used to integrate the equations of motion. The impact process is modeled during finite time by an equivalent linear spring and viscous damper representing, respectively, material deformation and energy loss during primary and secondary mass impact. This work corroborates, by an independent method, the results of G.V. Brown and C.M. North[1] who used closed form solutions and modeled impact, in infinitesimal time, by a restitution model.

DEFINITION OF SYMBOLS

ENGLISH SYMBOLS

A = Dimensional primary mass wall thickness.

C = Dimensional viscous damping coefficient.

C_c = Dimensional critical damping coefficient.

C_M = Dimensional equivalent primary mass damping coefficient.

d = Dimensional secondary mass width.

D = Dimensional cavity width.

e = Coefficient of restitution.

E = Dimensionless total system energy at any time t.

E_0 = Dimensionless initial total system energy.

$F(T)$ = Dimensional forcing function.

F_o = Dimensional forcing function amplitude constant.

$f_o = F_o/K\epsilon$ = Dimensionless forcing function amplitude constant.

K = Dimensional external elastic spring coefficient.

$k = K_M/K$ = Dimensionless equivalent primary mass spring coefficient.

K_M = Dimensional equivalent primary mass spring coefficient.

M = Dimensional primary mass.

m = Dimensional secondary mass.

T = Current dimensional time.

$t = \Omega_n T$ = Current dimensionless time.

X = Dimensional primary mass displacement.

dX/dT = Dimensional primary mass velocity.

d^2X/dT^2 = Dimensional primary mass acceleration.

$x = X/\epsilon$ = Dimensionless primary mass displacement.

x_0 = Dimensionless primary mass initial displacement at t = 0.

$dx/dt = (dX/dT)/\epsilon\Omega_n$ = Dimensionless primary mass velocity.

$d^2x/dt^2 = (d^2X/dT^2)/\epsilon(\Omega_n)^2$ = Dimensionless primary mass acceleration.

dx_0/dt = Dimensionless primary mass initial velocity at time t = 0.

Y = Dimensional secondary mass relative displacement.

dY/dT = Dimensional secondary mass relative velocity.

d^2Y/dT^2 = Dimensional secondary mass relative acceleration.

$y = Y/\epsilon$ = Dimensionless secondary mass relative displacement.

$dy/dt = (dY/dT)/\epsilon\Omega_n$ = Dimensionless secondary mass relative velocity.

dy'/dt = Dimensionless secondary mass relative velocity immediately following impact in the restitution equation.

$d^2y/dt^2 = (d^2X/dT^2)/\epsilon(\Omega_n)^2$ = Dimensionless secondary mass relative acceleration.

dy_0/dt = Dimensionless secondary mass initial relative velocity at time t = 0.

Z = Dimensional secondary mass absolute displacement.

dZ/dT = Dimensional secondary mass absolute velocity.

d^2Z/dT^2 = Dimensional secondary mass absolute acceleration.

$z = Z/\epsilon$ = Dimensionless secondary mass absolute displacement.

$dz/dt = (dZ/dT)/\epsilon\Omega_n$ = Dimensionless secondary mass absolute velocity.

$d^2z/dt^2 = (d^2Z/dT^2)/\epsilon(\Omega_n)^2$ = Dimensionless secondary mass absolute acceleration.

GREEK SYMBOLS

δ = Logarithmic decrement.

ϵ = D - d = Dimensional maximum secondary mass undeformed cavity travel.

η = Loss factor.

ν = m/M = Mass ratio.

Ω_f = Dimensional sinusoidal forcing function natural frequency.

Ω_m = $(K_M/M)^{0.5}$ = Dimensional primary mass material natural circular frequency.

Ω_n = $(K/M)^{0.5}$ = Dimensional system natural circular frequency.

Ω_s = $[K/(M + m)]^{0.5}$ = Dimensional stuck system natural circular frequency.

ω_f = Ω_f/Ω_n = Dimensionless sinusoidal forcing function natural circular frequency.

ω_m = Ω_m/Ω_n = $(k/\nu)^{0.5}$ = Dimensionless natural circular frequency or the primary mass material.

ω_n = Ω_n/Ω_n = 1 = Dimensionless harmonic oscillator natural circular frequency.

ω_s = Ω_s/Ω_n = $[1/(1+\nu)]^{0.5}$ = Dimensionless natural circular frequency of the stuck primary and secondary masses.

ζ = C/C_c = Damping ratio.

ζ_m = C_M/C_c = Hysteretic damping ratio.

ζ_s = C/C_c = Dimensionless stuck damping ratio.

1. INTRODUCTION

DESCRIPTION OF THE IMPACT DAMPER

The impact damper, known also as an acceleration damper or rattle damper, is a passive type mechanical damper. It consists of an oscillator containing a secondary mass which is able to travel freely between two stops either mounted directly to the oscillator (primary mass) or between opposite walls inside a hollow cavity within the primary mass.

The system is excited either by a forcing function or a nonzero set of initial conditions (displacement and velocity). Vibratory motion of the system causes the secondary mass to strike the stops or cavity walls of the primary mass introducing energy dissipation in the form of elastic waves, heat and noise.

Practical use of impact damping includes any application where its simplicity and reliability are required. One example is space station vibrations. Impact damping is unaffected by the cold vacuum of space and would require little maintenance. A second possible application is in turbomachinery. Implementation of impact damping in turbine blades and for rotor torsional vibration would not require external structural modification.

HISTORICAL DEVELOPMENT OF IMPACT DAMPING

Publications as early as 1833 exist in the literature. The first comprehensive analysis seems to have been reported in 1945 by P. Lieber and D.P. Jensen (see P.J. Soller's[2] chronology) using a forced plastic impact model without external damping. Various studies were performed until S.F. Masri in 1969 demonstrated both analytically and experimentally that two equally spaced impacts per cycle did exist (see P.J. Soller[2]). After this, analysis of the single degree of freedom system declined because coverage of this system was thought to be adequate.

In 1982 C.M. North, while working as a Summer Faculty Fellow at NASA Lewis Research Center, initiated the study of the transient motion of the impact damped simple harmonic oscillator. In a later study he added Coulomb friction between the primary and secondary masses. Under the direction of C.M. North, S.E. Pyle[4] in 1983 modeled the transient motion of a simple harmonic oscillator containing a viscous fluid as well as a secondary mass inside the cavity. These studies showed that the energy removed from the system by friction or by the presence of a viscous fluid was insignificant compared to that removed by impact damping.

Under the direction of C.M. North, P.J. Soller[2] in 1985 did a transient analysis of the externally forced and viscously damped harmonic oscillator with a single impact damper. His work checked the results of previous studies and reported the effect of mass ratio and coefficient of restitution on amplitude of vibration and duration of transient response.

In 1987, G.V. Brown and C.M. North[1] reported the results of a transient free decay time history solution of the impact damped simple harmonic oscillator. Their work showed that all the important characteristics of impact damping could be determined from a single transient free decay, precluding the need of a long term forced motion study. They reported three behavior ranges:

1.) a low amplitude range with less than one impact per cycle resulting in very low impact damping;
2.) a useful middle amplitude range with a finite number of impacts per cycle;
3.) a high amplitude range with an infinite number of impacts per cycle and progressively decreasing impact damping with increase in amplitude.

P.J. Torvik and W. Gibson[3], in 1987, parametrically investigated the impact damper analytically and experimentally. Their work compared analytical predictions to experimental results.

In 1988, under the direction of C.M. North, T.A. Nale[5] reported the study of the transient free decay motion of the impact damped cantilever beam. This model explored the influence of cavity location, secondary mass travel, and the higher modes on the effects of impact damping. The results revealed that cavity location and secondary mass travel can be used to optimize the damper effects on vibration amplitude. Of significance was the fact that the first mode proved to be predominant in influencing the vibratory motion of the beam, and consequently, higher modes are not required to produce an accurate assessment of the effects of the impact damper.

OBJECTIVE OF THIS STUDY

The primary objective of this study is to evaluate the effectiveness of the Component Element Method[6] in modeling the transient free decay response of the viscously damped, simple harmonic oscillator. The method models material deformation during finite time of impact with the internal impact damper. The evaluation is made by comparison of results obtained with the previous work of G.V. Brown and C.M. North[1].

COMPONENT ELEMENT METHOD DESCRIPTION

Springs, masses and dampers comprise an assemblage of elementary components. The Component Element Method[6] uses a finite difference step-by-step process of integrating the equations of motion of the assemblage. Because of this feature, system complexity is not limited by the ability to find closed form solutions as it is when using purely analytical methods.

The method chosen here for approximating derivatives by finite differences is the central difference approximation. As long as the time interval chosen is kept within $2(\pi)/\omega_n$, where ω_n is the highest natural frequency (rad/sec) in the system, the solutions will be accurate and converge to the exact solution (see Levy et al.[6]).

2. SYSTEM MATHEMATICAL MODEL

PHYSICAL SYSTEM

The modeled system is a simple harmonic oscillator with one internal impact damper with optional viscous damping and an optional sinusoidal forcing

forcing function. The sliding contact surfaces between the primary and secondary masses are assumed to be frictionless. The configuration shown in Fig. A is the dimensional representation of the system. The absolute displacement of the primary mass M is X. The relative and absolute displacements of the secondary mass m are Y and Z, respectively. The corresponding external spring and viscous damping coefficients are K and C, respectively. The sinusoidal force F(T) is a function of real time T. The primary mass cavity wall thickness is A. The cavity width is D and d is the width of the secondary mass.

The free decay motion in this study begins at dimensionless time zero. The primary mass is released from rest with an initial dimensionless displacement of 6.0. All other initial values of relative displacement and velocity are 0.0. The primary mass equivalent material components, K_M and C_M represent, respectively, the material deformation and structural damping of the primary mass as it undergoes impact with the secondary mass (see L. Meirovitch[7] and G.K. Hobbs[8]). Although the secondary mass also deforms and registers energy loss due to hysteresis damping, these losses are lumped into the equivalent spring and viscous damper shown schematically in Fig. A as a part of the primary mass cavity wall.

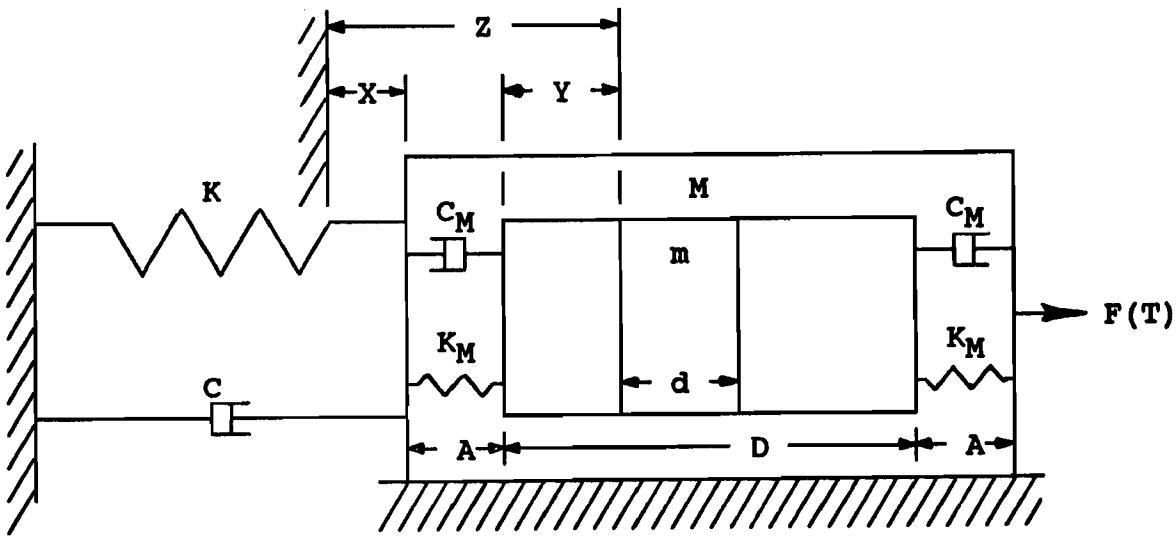

Figure A System Configuration in Free Motion

PRESENT MODEL DESCRIPTION

The model developed here uses the numerical method of finite difference with central difference approximations to integrate, with respect to time, the equations of motion of the primary and secondary masses.

Free motion is the condition where the two masses are experiencing frictionless sliding contact, but without contact between the secondary mass and the cavity wall of the primary mass.

The impact model at the cavity walls accounts for the deformation, energy, displacement, velocity, and acceleration changes that occur during a finite time of impact.

The elastic deformation of the primary mass during impact with the

secondary mass is modeled by an equivalent linear spring whose material elastic modulus is K_M. Assumptions are:

1.) the material is linearly elastic;
2.) no permanent deformation occurs;
3.) the secondary mass is small compared to the primary mass;
4.) the deformations of the primary mass cavity walls due to impact with the secondary mass are small compared to the secondary mass travel ϵ within the cavity.

Resultant hysteretic damping due to impact with the secondary mass is modeled as an equivalent linear viscous damper whose damping coefficient is C_M and whose damping ratio, ζ_m, is determined iteratively by a subroutine contained in a FORTRAN computer model. This subroutine models the deformation and energy loss from a collision between the motionless primary mass and the secondary mass by simulating the impact between a secondary mass m of unit velocity and a spring damper pair like the one shown in Fig. B. The spring is the equivalent linear spring whose elastic modulus is K_M and the damper is the equivalent linear viscous damper whose damping coefficient is C_M.

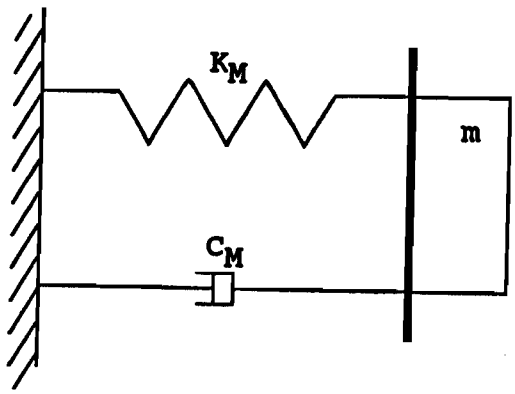

Figure B Iterative Impact Model

The subroutine uses the known values of the dimensionless spring elastic modulus, k, coefficient of restitution, e, and initial unit impact velocity of the mass m. Closed form solutions are used to step through the impact process beginning with a small assumed value of the structural damping ratio ζ_m. A minimum of one hundred steps is used to assure accuracy of ζ_m within an error of 10^{-8}. At the conclusion of impact the secondary mass m has returned to the impact starting position and its relative velocity is checked against the relative velocity provided by the restitution model. If the velocities do not agree within the error of 10^{-8}, ζ_m is changed iteratively until the restitution model is satisfied to within the required tolerance.

A phenomenon called "bounce-down" appears in a time study of a sufficiently excited impact damped system. Bounce-down commences when the secondary mass fails to acquire the velocity necessary to reach the opposite cavity wall before colliding again with the previously impacted cavity wall.

In free decay bounce-down will always terminate in the stuck regime (definition to follow).

Bounce-down impact frequency rapidly increases while relative displacement amplitude decreases. This motion continues until separation of the two masses ceases to occur. Their motion, however, continues as minute deformation induced oscillations without physical separation until hysteretic damping dissipates the deformation induced oscillatory motion. This is analogous to dropping a ball on a sidewalk and letting it bounce to a stop.

Bounce-down ends and the "stuck" condition begins when the secondary mass relative velocity and relative acceleration become zero. The secondary mass adheres to and moves with the primary mass until primary mass acceleration changes sign reducing the normal reaction between the masses to zero. At that point the secondary mass no longer adheres to the primary mass, but is "slung" free, initiating a free motion regime.

In free decay when the primary mass dimensionless amplitude diminishes from its initial value of 6.0 to an approximate value of 5.0, bounce-down and the associated stuck condition cease to occur. Subsequently, the number of impacts per half cycle decreases with decreasing dimensionless primary mass peak amplitude until less than one impact per half cycle is recorded. This point in the time history is called "Impact Failure" and designates the loss of damping effectiveness of the impact damper.

DIMENSIONLESS EQUATIONS OF MOTION

To obtain results in a general form with the widest applicability the equations of motion are made dimensionless as shown below. (See R.E. Jones[9] for the complete derivation.)

Time is made dimensionless with respect to the reciprocal of the primary mass undamped natural circular frequency (which is the period of the undamped primary mass motion). The circular frequency $\Omega_n = (K/M)^{0.5}$. The corresponding dimensionless time is

$$t = \Omega_n T. \tag{1}$$

Displacements are made dimensionless with respect to the secondary mass free travel $\epsilon = D - d$ within the cavity. The dimensionless displacements x, y, z are: $x = X/\epsilon$, $y = Y/\epsilon$, $z = Z/\epsilon$. By letting $\omega_f = \Omega_f/\Omega_n$ and $f_o = F_o/(K\epsilon)$ the Sinusoidal forcing function can be written in the dimensionless form

$$F(T)/(K\epsilon) = f_o \sin(\omega_f t). \tag{2}$$

FREE MOTION MODEL

Free motion is the resulting motion of the primary and secondary masses when they are not impacting. The equations of free motion for the primary and secondary masses are well known (see R.K. Vierck[10], or S.S. Rao[11]). The dimensionless equations of free motion for the primary and secondary masses are,

$$d^2x/dt^2 + 2\omega_n\zeta(dx/dt) + (\omega_n)^2 x = f_o \sin(\omega_f t) \tag{3}$$

$$d^2y/dt^2 = -d^2x/dt^2 \tag{4}$$

IMPACT MODEL

The primary mass experiences deformation of the cavity wall due to secondary mass impact. The normal force between the two masses is non-zero. The dimensionless equations of motion for impact at the left cavity wall are:

$$d^2x/dt^2 + 2\omega_n\zeta(dx/dt) + (\omega_n)^2x = \nu[2\omega_m\zeta_m(dy/dt) + (\omega_m)^2y] + f_o\sin(\omega_f t) \quad (5)$$

$$d^2y/dt^2 + 2\omega_m\zeta_m(dy/dt) + (\omega_m)^2y = -d^2x/dt^2 \quad (6)$$

The dimensionless equations of motion for impact at the right cavity wall are:

$$d^2x/dt^2 + 2\omega_n\zeta(dx/dt) + (\omega_n)^2x = \nu[2\omega_m\zeta_m(dy/dt) + (\omega_m)^2(y - 1)] + f_o\sin(\omega_f t) \quad (7)$$

$$d^2y/dt^2 + 2\omega_m\zeta_m(dy/dt) + (\omega_m)^2(y - 1) = -d^2x/dt^2 \quad (8)$$

STUCK MODEL

In the stuck regime the two masses are in contact but the normal force between them is not zero. This condition results in the same equation of motion when the secondary mass is stuck at either cavity wall. The equations of motion for the stuck regime are:

$$d^2x/dt^2 + 2\omega_s\zeta_s(dx/dt) + (\omega_s)^2x = f_o\sin(\omega_f t) \quad (9)$$

$$d^2y/dt^2 = -d^2x/dt^2. \quad (10)$$

SYSTEM ENERGY ANALYSIS

The total dimensionless energy of the system at any time is the sum of the dimensionless kinetic and potential energy in the system.

$$E = 0.5\{(dx/dt)^2 + \nu[(dx/dt)^2 + (dy/dt)^2] + x^2\}$$

The ongoing percent of system energy at any time is determined by dividing the current system energy by the initial system energy,

$$E_0 = 0.5\{(dx_0/dt)^2 + \nu[(dx_0/dt)^2 + (dy_0/dt)^2] + (x_0)^2\}.$$

3. ANALYSIS OF COMPUTER RESULTS

GENERAL COMMENTS

This work used the numerical technique of finite differences to integrate the equations of motion (3) - (10) in a FORTRAN 77 computer program to generate the transient time history of the viscously damped simple harmonic oscillator with impact damping.

When the dimensionless primary mass displacement is greater than approximately 5.0 (mass ratio $\nu = 0.02$, coefficient of restitution $e = 0.6$, and viscous the damping ratio $\zeta = 0.0$) the secondary mass experiences the

bounce-down phenomenon that in free decay always terminates in the stuck condition. The greater the dimensionless primary mass peak amplitude the shorter the time duration that the secondary mass spends in the bounce-down condition and the greater the time duration it is stuck to a cavity wall of the primary mass. To prevent a lengthy stay in the bounce-down and stuck conditions (which occurred in G.V. Brown and C.M. North[1] where the initial dimensionless primary mass displacement was 10.0) the initial dimensionless primary mass displacement was set here at 6.0. At the end of bounce-down and the stuck regime, the number of impacts per half cycle that the secondary mass experiences on one cavity wall before gaining sufficient relative velocity to impact with the opposite cavity wall decreases with diminishing dimensionless amplitude. This decline in number of impacts per half cycle continues until impact failure ensues when less than one impact per half cycle occurs at an approximate dimensionless amplitude between 0.1 and 0.05. The range of greatest damping effectiveness for the impact damper lies between bounce-down termination and impact failure. It is in this regime of primary mass amplitude that the secondary mass acquires its greatest relative velocity due to impacts on the advancing cavity wall. Structural damping is represented here by an equivalent viscous damper. Therefore, damping is a function of the relative velocity between the primary and secondary masses. As the absolute value of the dimensionless primary mass peak amplitude decreases, dimensionless secondary mass relative velocity increases faster than the dimensionless primary mass velocity decreases, resulting in an increase in the relative velocity between the two masses. Thus the high relative velocity between the two masses due to impacts on approaching cavity walls is responsible for the high rate of impact damping effectiveness.

All the results discussed here were generated from the output files of a computer program whose source code and executable file are stored on the accompanying diskette of R.E. Jones[9]. Figures 1 - 6 were made directly from these computer output files where the mass ratio $\nu = 0.02$, the coefficient of restitution $e = 0.6$ and viscous damping ratio $\zeta = 0.0$. All "Dimensionless Amplitude" data plotted on the ordinate of Fig. 7 and the abscissas of Figures 8 - 14 were generated from the absolute values of the dimensionless peak primary mass displacement at each half cycle of the primary mass motion. In Fig. 15 the "Dimensionless Amplitude" is the peak primary mass dimensionless amplitude that occurs during the half cycle in which an impact or impacts may also occur. Therefore one value of dimensionless amplitude may apply to several impacts. This is not to be confused with the dimensionless amplitude of the primary mass at the time of the impact.

SYSTEM MOTION

The secondary mass experiences several types of motion from bounce-down to impact failure. Three of these motion geometries (relative to the cavity walls) are shown in Figures 1 - 3 which occur at approximate primary mass dimensionless amplitudes of 5.6, 2.6, 0.6, respectively. Fig. 1 illustrates the bounce-down condition followed by the stuck regime. Later on, after bounce-down ceases, the secondary mass in Fig. 2 is impacting a cavity wall three times before gaining sufficient relative velocity to cross the cavity travel width to the opposite cavity wall. Even later in the time history, in Fig. 3, the secondary mass impacts a cavity wall twice before alternating with a single impact on the opposite cavity wall.

In Figures 4 - 6 the approximate primary mass dimensionless amplitudes are 0.4, 0.2, 0.05, respectively. The dimensionless secondary mass absolute displacement is represented by a dashed line and the absolute displacement of the two cavity walls is represented by two solid lines. Two unequally spaced impacts per cycle are shown in Fig 4. Later in the free decay, two equally spaced impacts per cycle are shown in Fig. 5. Fig. 6 clearly exhibits the point where the impact damper loses its effectiveness when impact failure begins.

LOSS FACTOR

The loss factor is a measure of damping effectiveness, where the greater the loss factor, the more effective the damper is at reducing the primary mass vibratory motion. The loss factor is defined as the change in primary mass energy that occurs between the two extreme absolute dimensionless primary mass displacement peaks of a cycle divided by the primary mass energy at the absolute dimensionless primary mass half cycle peak that lies midway between the two full cycle peaks; i.e., the loss factor is

$$\eta = \Delta E/E,$$

where E is the total system energy. When the simple harmonic oscillator is at a peak amplitude, the kinetic energy vanishes and the total energy is:

$$E = kx^2/2$$

Since $\Delta E = kx\Delta x$ then the loss factor per cycle is:

$$\eta = 2\Delta x/x$$

AVERAGED LOSS FACTOR

To generate the "Averaged Loss Factor" each point of the data shown in Figures 8 - 14 is the result of a least squares parabolic fit applied to the absolute values of primary mass peak amplitudes for ten successive half cycles (eleven data points). These data are used to determine the averaged loss factor. This smoothing or averaging is necessary because of the variations in peak amplitudes. Some data required the application of the least squares fit to as many as 18 half cycles in order to present the data in acceptably smooth form. The averaging process has the effect of broadening and reducing the loss factor peaks.

In Figures 8 - 15 the primary mass dimensionless displacement amplitudes are decreasing as the free decay time history progresses.

AMPLITUDE DECAY

Fig. 7 displays the decay curves of the absolute value of the dimensionless peak half cycle amplitudes versus the time of the amplitude occurrence. For this figure the external damping ratio $\zeta = 0.0$, and mass ratio is $\nu = 1, 2, 4$ percent, while all other parameters are held constant. The efficiency of impact damping for a given set of parameters corresponds to the slope of the curve. Clearly illustrated is the increase in loss factor

with decrease in amplitude until impact failure commences at a dimensionless amplitude of between approximately 0.05 - 0.1. Impact failure is easily recognized here by the curve tails close to the horizontal axis. The bounce-down and stuck regime is in the dimensionless primary mass amplitude range above approximately 5.0.

EFFECTS OF THE MASS RATIO

In Fig. 8 the coefficient of restitution, e = 0.6, external damping ratio $\zeta = 0.0$, and three values of mass ratio, $\nu = 1, 2, 4$ percent are used to demonstrate the increase in loss factor with a decrease in amplitude. Comparing Fig. 8 with Figures 4 and 5 indicates that maximum damping efficiency due to impact damping occurs when the secondary mass experiences one impact per half cycle. The similarity between the curves depicted in Fig. 8 suggests a factor may exist, when applied to each curve, that would cause the three to converge on one common curve. The curves in Fig. 8 are reduced nearly to a single curve as shown in Fig. 9 by dividing the averaged loss factor by the mass ratio (also called the "Specific Total Loss Factor"). The specific total loss factor is a constant at any given amplitude for mass ratios up to 4 percent. This demonstrates that the loss factor and the dissipated energy due to impact (Fig. 8) are approximately proportional to the mass ratio.

EFFECTS OF VISCOUS DAMPING

Fig. 10, with a single value of the coefficient of restitution e = 0.6 and mass ratio of $\nu = 2$ percent, compares the loss factors resulting from viscous damping ratios of 0.0, 0.2, 0.4, 0.8 percent.

The "Specific Secondary Mass Loss Factor" is obtained when the damping contribution made by twice the viscous damping ratio 2ζ is subtracted from the averaged loss factor in Fig. 10, and the result is divided by the mass ratio. This contribution of viscous damping 2ζ is obtained from the logarithmic decrement, δ, which is a measure of the rate of decay between any two successive cycles (for detailed derivation, see R.E. Jones[9]).

The simple additive nature of viscous and impact damping is illustrated in Fig. 11. The nearly identical overlapping curves show that viscous damping on the primary mass and impact damping are additive for very small viscous damping ratios. This near coincidence of the curves provides a single curve that closely describes the specific secondary mass loss factor as a function of dimensionless amplitude. However, this curve is unique for the value of the coefficient of restitution e = 0.6. Different curves can be generated for other values of the coefficient of restitution. Over most of the length of the curve, the specific secondary mass loss factor increases as the dimensionless amplitude decreases.

Fig. 12 illustrates to what extent the apparent approximate correspondence between amplitude and the specific secondary mass loss factor exists in Fig. 11. To show this the specific secondary mass loss factor from Fig. 11 is multiplied by the dimensionless amplitude. The resulting overlapping of the curves justify the correspondence. In the dimensionless amplitude range from 0.1 - 6.0 the curve has variations within ±31 percent of the average ordinate value 0.339. The approximate constant value of the ordinate provides an easy estimate of impact damping over a wide amplitude

range.

EFFECTS OF THE COEFFICIENT OF RESTITUTION

The general effect of changing the coefficient of restitution e is shown in Fig. 13. The dimensionless amplitude multiplied by the specific secondary mass loss factor is represented for values of e = 0.4, 0.6, 0.8 and mass ratio ν = 2 percent, and viscous damping ratio ζ = 0.0. The lower value of e = 0.4 results in increased loss factor in the middle dimensionless amplitude range of 0.1 to bounce-down termination. Bounce-down ends at approximately 2.0 and 5.0 for coefficients of restitution e = 0.4 and 0.6, respectively. For coefficient of restitution e = 0.8 bounce-down ends at an amplitude beyond the scope of this study (greater than 6.0). For coefficients of restitution values of e = 0.4, 0.6, 0.8, impact failure begins at approximately 0.15, 0.1 and 0.01, respectively. To summarize, for lower values of the coefficient of restitution, e, bounce-down ends at lower dimensionless amplitudes and impact failure begins at higher values of the dimensionless amplitude. Higher values of the coefficient of restitution e have just the opposite effect.

Fig. 14 is obtained from Fig. 13 by dividing the ordinate values in Fig. 13 by (1 - e). The merging of the curves demonstrates that within impact damping active range (implied by Fig. 13), the damping is approximately proportional to (1 - e).

IMPACT PHASE ANGLE

Fig. 15 is a phase plot (without viscous damping) of the secondary mass impacts that occur during a half cycle where the dimensionless primary mass amplitude is the absolute value of the dimensionless primary mass peak amplitude in a half cycle. The coefficient of restitution e = 0.6 and the mass ratio ν = 0.02. The phase angle in degrees is determined from the secondary mass cavity wall impact point between primary mass crossings of the zero dimensionless displacement axis. A half cycle of 180 degrees is defined between the dimensionless primary mass displacement amplitude zero crossings. The secondary mass impact phase in degrees is defined by the point in time at which the impact of the secondary mass occurs during the dimensionless primary mass displacement half cycle. This point is established when the dimensionless secondary mass relative displacement is zero (impact at the left cavity wall) or one (impact with the right cavity wall). The relationship is

$$\text{Phase} = \frac{\text{Time from last zero crossing to impact}}{\text{Time between zero crossings}} \times 180°.$$

The initial time for the data shown in Fig. 15 corresponds to the initial dimensionless amplitude of 6.0 and the time history progresses as amplitude decreases. Impact points are shown in the figure as small squares. The darkened area in the upper right corner of the figure represents the stuck regime where the secondary mass moves in temporary contact with the primary mass until the dimensionless primary mass acceleration changes sign. The area beneath the stuck region all the way down to the horizontal axis is the realm of bounce-down. Notice that in the bounce-down region the impact phase (at a given dimensionless amplitude) increases as the stuck regime is approached

vertically from the horizontal axis until bounce-down terminates in the stuck regime. At an approximate dimensionless amplitude of 5.0 bounce-down and the stuck regime cease. At that point, as the dimensionless amplitude diminishes, the number of impacts per half cycle also diminishes. Note that at progressively decreasing amplitudes of approximately 4.4, 4.0, 3.3, 2.5, 1.3, 0.2 in Fig. 15, clear patterns of six, five, four, three, two, and one impacts per half cycle, respectively, are indicated. The plot clearly shows that regular impact regions per half cycle alternate with regions of chaotic impact. Comparing Fig. 15 with the slopes of the curves in Fig. 7, impact damping is seen to be most efficient (for coefficient of restitution e = 0.6 and mass ratio ν = 0.02) in the region of single impacts per half cycle. This corresponds to a dimensionless amplitude range from approximately 0.2 to impact failure, which ensues at approximate dimensionless amplitudes of 0.05 - 0.1.

4. COMPARISON OF RESULTS TO THOSE OF G.V. BROWN AND C.M. NORTH[1]

SIMILARITIES AND DIFFERENCES

In comparing these results with those of the previous work of G.V. Brown and C.M. North[1], the observable differences can be attributed to:

1. the inherent difference between the two models;
2. initial conditions;
3. a variation in the least squares method used for loss factor averaging.

Although all the results compare well, close scrutiny shows a very small difference in data point to data point comparison. During one comparative run of identical parameters the dimensionless time required for reducing vibratory motion from initial primary mass displacement to impact failure was approximately 5 - 10 percent less here than in G.V. Brown and C.M. North[1]. However, more study should be performed to verify this observation. Also the chaotic regions appear to be less chaotic in Fig. 15 than in G.V. Brown and C.M. North[1].

G.V. Brown and C.M. North[1] began the free decay time history at a dimensionless primary mass displacement amplitude of 10.0. The present study initiated free decay with a dimensionless primary mass displacement amplitude of 6.0. The larger of these two amplitudes causes the primary and secondary masses to remain in the bounce-down and stuck regime for a longer length of time for all of the results presented. As a consequence, their time histories will always require longer dimensionless times to reach impact failure since more time was spent in the bounce-down and stuck regimes where small damping occurs.

In each of the loss factor curves (Figures 8 - 12) a maximum value peak in the region of impact failure is lower and broader here than in G.V. Brown and C.M. North[1]. The peak in question is located at a dimensionless amplitude of approximately 0.1 in Figures 8 - 12. In Figures 13 and 14 the peak corresponding to each of the three curves in each figure occurs at dimensionless amplitude of approximately 0.08, 0.1, 0.12. G.V. Brown and C.M. North[1] used a variation of the loss factor averaging scheme in the vicinity of

this peak causing the difference in appearance of the curve in the two works. It is noted however, that the region of impact failure appears to contain little meaningful information.

SUMMARY

The overall results given here are qualitatively identical to G.V. Brown and C.M. North[1]. This similarity of results from the two studies supports the assumptions of G.V. Brown and C.M. North[1] while lending credibility to the model in the present work. The present work uses finite differences with central difference approximations to integrate the equations of motion. The actual impact process is modeled using discrete time intervals during impact between the primary and secondary mass. The deformation and energy losses of the impacting masses are assumed to be equivalent to a linear spring and viscous damper, respectively, for the small deformations involved. G.V. Brown and C.M. North[1] used closed form solutions and initiated free decay with a dimensionless primary mass initial displacement of 10.0. The coefficient of restitution was used to model across impact by assuming the time duration of impact to be infinitesimally small compared to the time required for the secondary mass to travel between impacts. The differences between these basic models accounts for all of the deviations between the results obtained from the two studies.

5. CONCLUSIONS

The accuracy of the numerical method is dependent directly on the size of the time step used. The smaller the time step, the more accurate the results. The spring and damper components used are all assumed to be linear and subject to linear restrictions (e.g., small deformations). The equivalent linear damper used to simulate structural damping is viscous and it is therefore velocity dependent. Structural damping is typically nonlinear and dependent upon the magnitude of deformation. For small secondary mass to primary mass ratios, the justification for using the more convenient viscous damping for a structural damping model comes from assuming small structural deformations resulting from impacts between the primary and secondary masses.

The component element method with its utilization of the numerical finite difference technique is shown to be a useful analysis tool for investigating the impact damped simple harmonic oscillator in freely decaying motion. The impact process is modeled as if the deformation and energy losses from the impacting primary and secondary masses were replaced by an equivalent linear spring and viscous damper. The results obtained have been shown to compare favorably, for small mass ratios, to G.V. Brown and C.M. North[1] who used closed form solutions to model the motion and a restitution model across impact. The accuracy of the results make the component element method worth consideration for future investigations of more complex systems of multiple components and impact dampers where closed form solutions may prove difficult or impossible to obtain. Although not utilized here, the component element method has the flexibility of incorporating nonlinear expressions or even data bases to represent component moduli.

The present computer model confirmed the following results obtained earlier by G.V. Brown and C.M. North[1]:

(1) A low amplitude and corresponding low effective impact damping range occurs for impact damping for coefficients of restitution e = 0.4, 0.6, 0.8. Impact failure is dominant for the diminishing dimensionless amplitudes starting at 0.15, 0.1, 0.01, respectively, where less than one impact per half cycle occurs.
(2) Between bounce-down and the stuck regime to the beginning of impact failure a middle dimensionless amplitude range of useful impact damping exists. The number of impacts per half cycle in this range depends on the dimensionless primary mass amplitude (i.e., the greater the amplitude the more impacts per half cycle).
(3) In the bounce-down and stuck regime impact damping is decreasingly effective. Dimensionless primary mass amplitudes are above approximately 2.0 and 5.0 for coefficients of restitutions e = 0.4, 0.6 respectively. The number of impacts per half cycle is large and can increase without bound as the coefficient of restitution approaches one.

For additional light viscous damping the impact damping in the middle dimensionless amplitude range from the bounce-down and stuck regime to impact failure is shown to be:

(1) represented by one curve for a given coefficient of restitution implying that impact damping is proportional to the mass ratio;
(2) additive to proportional viscous damping;
(3) a unique function of vibration amplitude where the loss factor increases as the dimensionless primary mass amplitude decreases;
(4) proportional to (1 - e), where e is the coefficient of restitution.

For a coefficient of restitution e = 0.6 and mass ratio ν = 0.02 impact damping is most effective when the dimensionless amplitude is about 10 percent of the secondary mass cavity travel (dimensionless value of one). The loss factor has a maximum value of nearly 0.1 and over a wide range of dimensionless amplitudes the loss factor is 0.01. Impact damping is a strong function of amplitude and produces substantial damping for small mass ratios. Because of this, several impact dampers may be combined with different secondary mass travel gaps to provide damping over wide ranges of amplitude.

6. REFERENCES

[1] Brown, G.V., C.M. North. "The Impact Damped Harmonic Oscillator in Free Decay," The Role of Damping in Vibration and Noise Control, ASME Publication, DE-Vol. 5, 1987, pp. 53-64.

[2] Soller, P.J. "The Development of a Computer Model as an Aid to the Solution of the Problem of Impact Damping," Masters Thesis, Rose-Hulman Institute of Technology, Terre Haute, IN, 1985.

[3] Torvik, P.J., W. Gibson. "The Design and Effectiveness of Impact Dampers for Space Applications." The Role of Damping in Vibration and Noise Control, ASME Publication, DE-Vol. 5,1987, pp. 53-64

[4] Pyle, S.E. "Computer Simulation of Internal Viscous Damping." Masters Thesis, Rose-Hulman Institute of Technology, Terre Haute, IN, 1983.

[5] Nale, T.A. "Time History Study of a Classical Cantilever Beam Damped by Internal Mechanical Means," Masters Thesis, Rose-Hulman Institute of Technology, Terre Haute, IN, 1988.

[6] Levy, S., J.P.D. Wilkinson. The Component Element Method In Dynamics, (New York, N.Y.: McGraw-Hill, 1976).

[7] Meirovitch, Leonard. Analytical Methods in Vibrations, (New York, N.Y.: Macmillan, 1967).

[8] Hobbs, G.K.. "Methods of Treating Damping in Structures," AIAA/ASME 12th Structures, Structural Dynamics and Materials Conference, ASME Publication, AIAA Paper No.71-347, 1971.

[9] Jones, R.E. "Application of the Component Element Method to the Impact Damped Simple Harmonic Oscillator," Masters Thesis, Rose-Hulman Institute of Technology, Terre Haute, IN, 1988.

[10] Vierck, R.K.. Vibration Analysis, Second Edition. (New York, N.Y.: Harper & Row, 1979).

[11] Rao, S.S.. Mechanical Vibrations, (Reading, MA: Addison-Wesley, 1986).

7. FIGURES

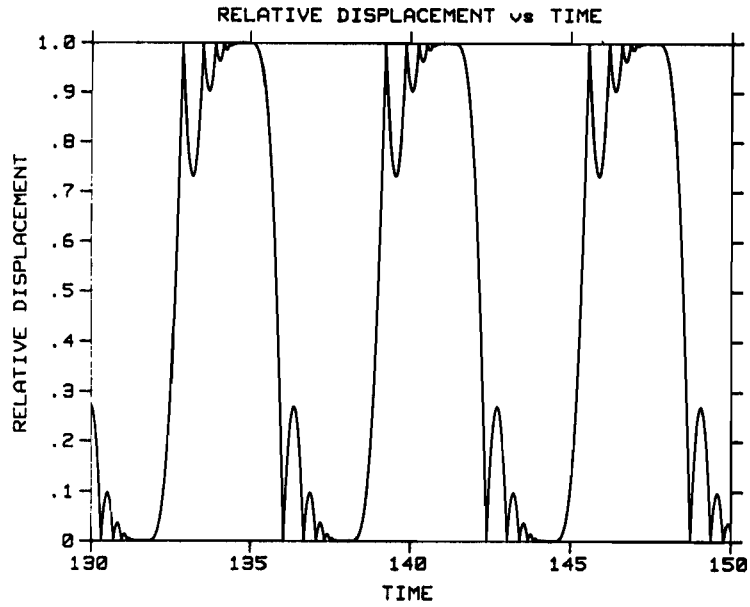

Figure 1 Large Number of Impacts in Each Half Cycle.

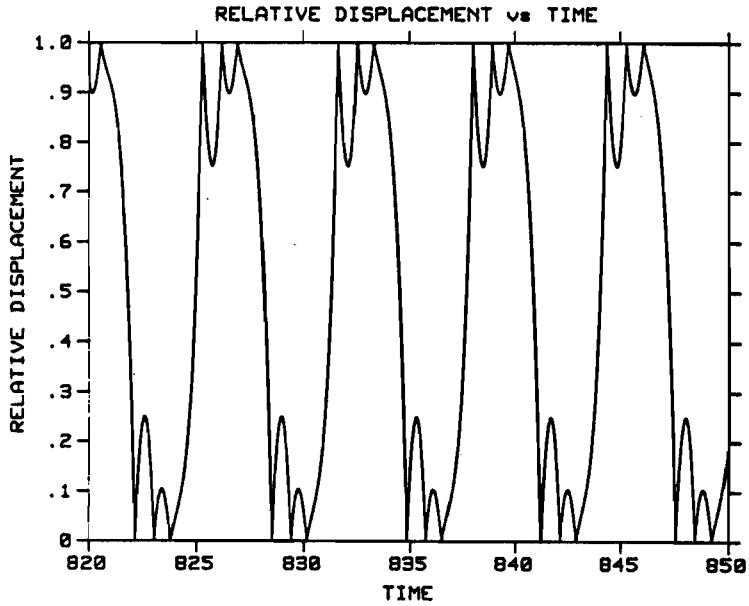

Figure 2 Three Impacts in Each half Cycle.

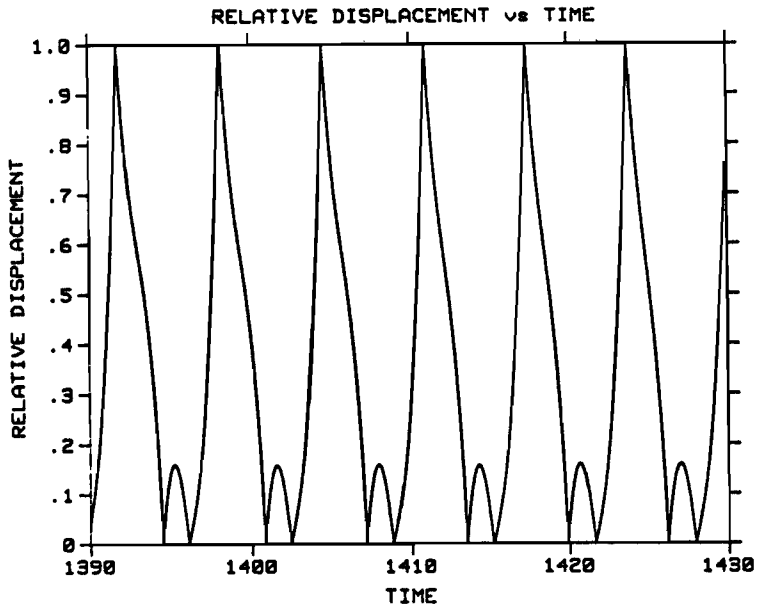

Figure 3 One Impact in Each Half Cycle Alternating with Two.

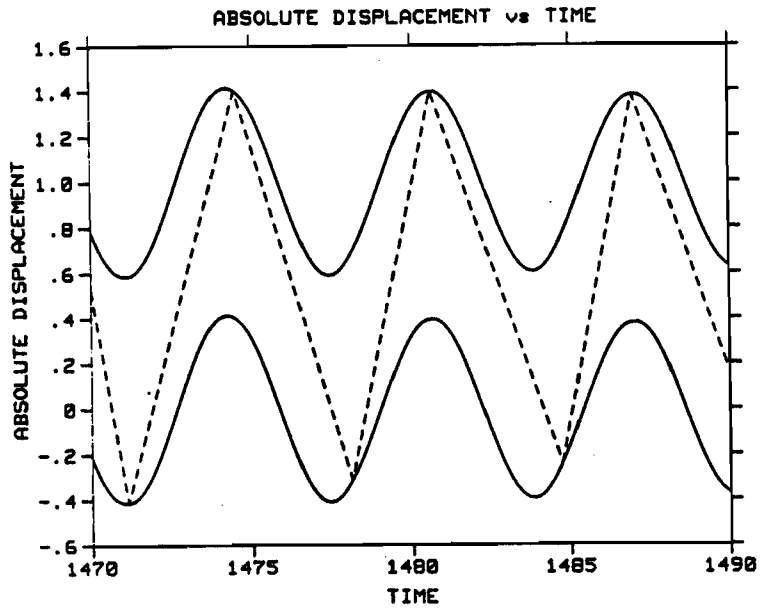

Figure 4 Two Unequally Spaced Impacts in Each Cycle.

KBA-20

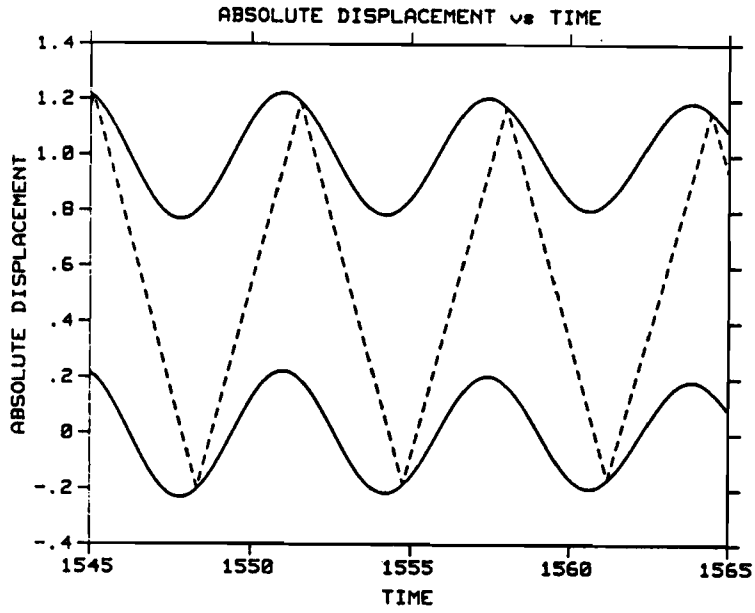

Figure 5 Two Equally Spaced Impacts in Each Cycle.

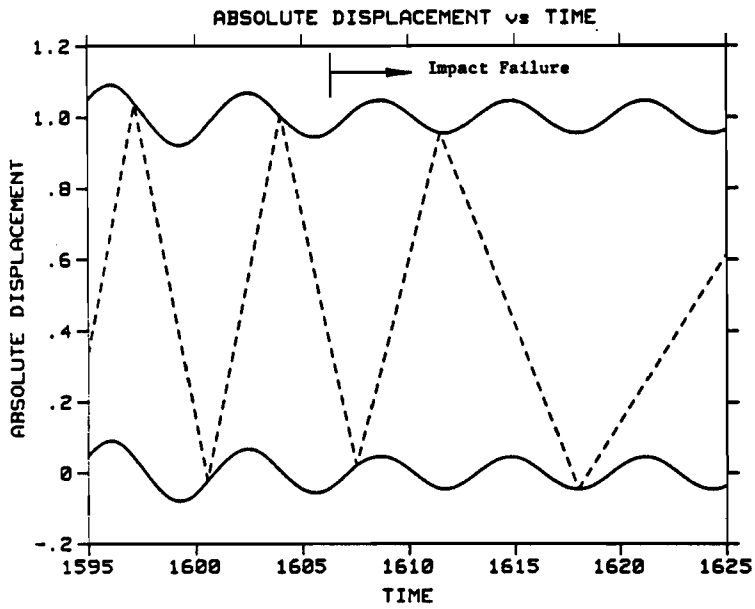

Figure 6 Beginning of Impact Failure.

KBA-21

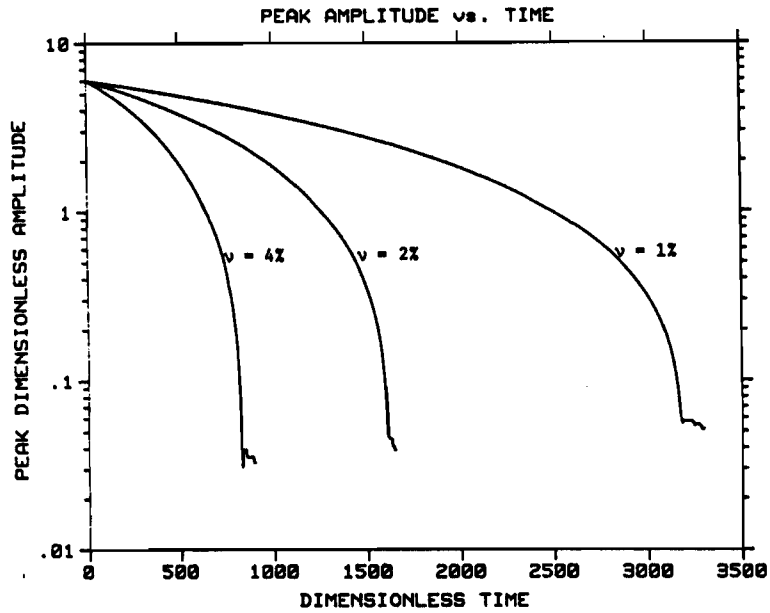

Figure 7 Amplitude Decay Curves. e = 0.6

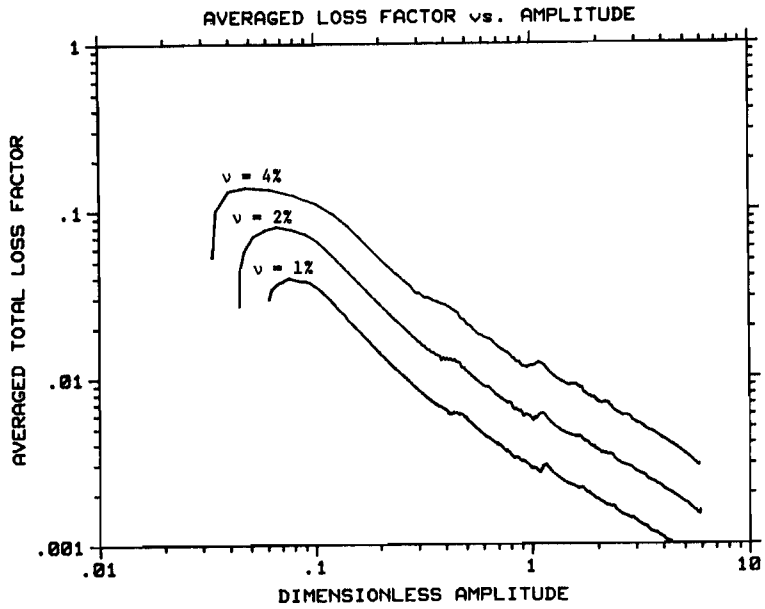

Figure 8 Averaged Total Loss Factor as a Function of Amplitude for Three Values of the Impactor Mass Ratio. e = 0.6; ν = 1, 2, 4 percent.

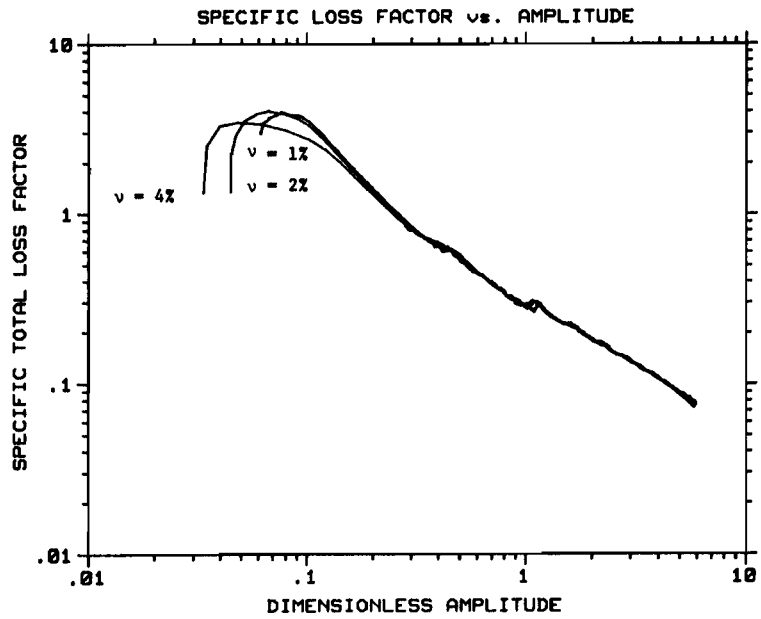

Figure 9 Specific Total Loss Factor as a Function of Amplitude for Three Values of the Impactor Mass Ratio e = 0.6; ν = 1, 2, 4 percent.

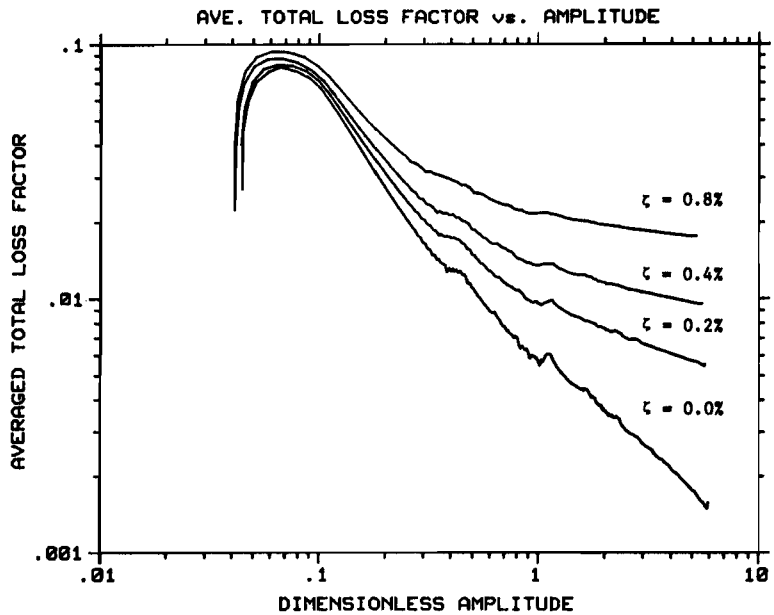

Figure 10 Averaged Total Loss Factor as a Function of Amplitude for Four Values of Viscous Damping Ratios. ν = 0.02; e = 0.6; ζ = 0.0, 0.2, 0.4, 0.8 percent.

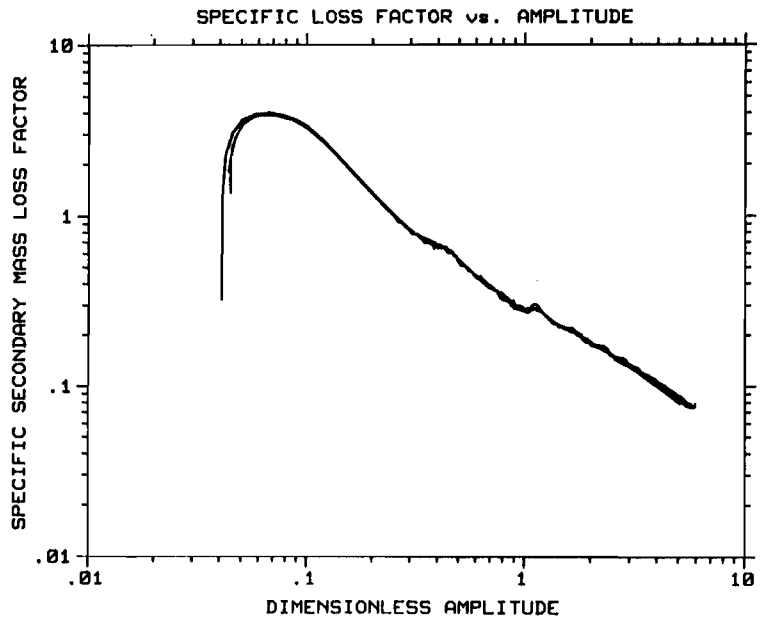

Figure 11 Specific Secondary Mass Loss Factor as a Function of Amplitude for Four Values of Viscous Damping Ratios. ν = 0.02; e = 0.6; ζ = 0.0, 0.2, 0.4, 0.8 percent.

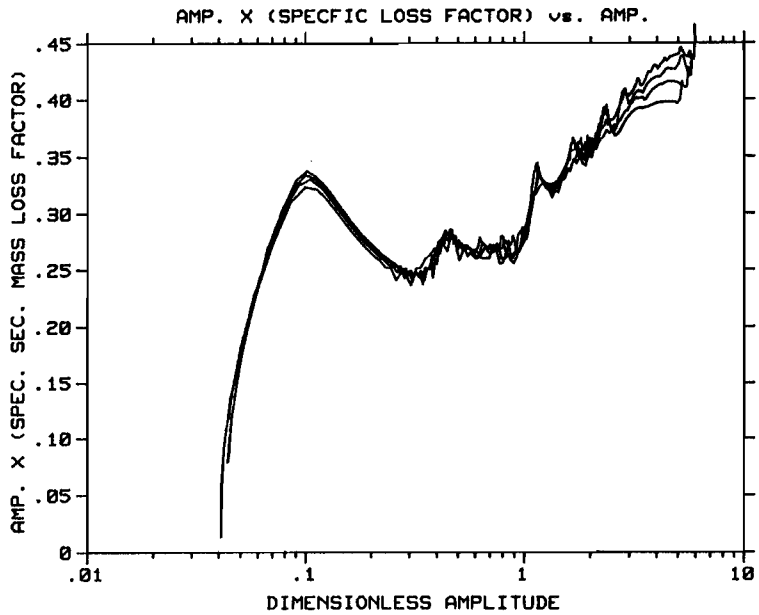

Figure 12 Amplitude Multiplied by the Specific Secondary Mass Loss Factor as a Function of Amplitude for Four Values of Viscous Damping Ratios. ν = 0.02; e = 0.6; ζ = 0.0, 0.2, 0.4, 0.8 percent.

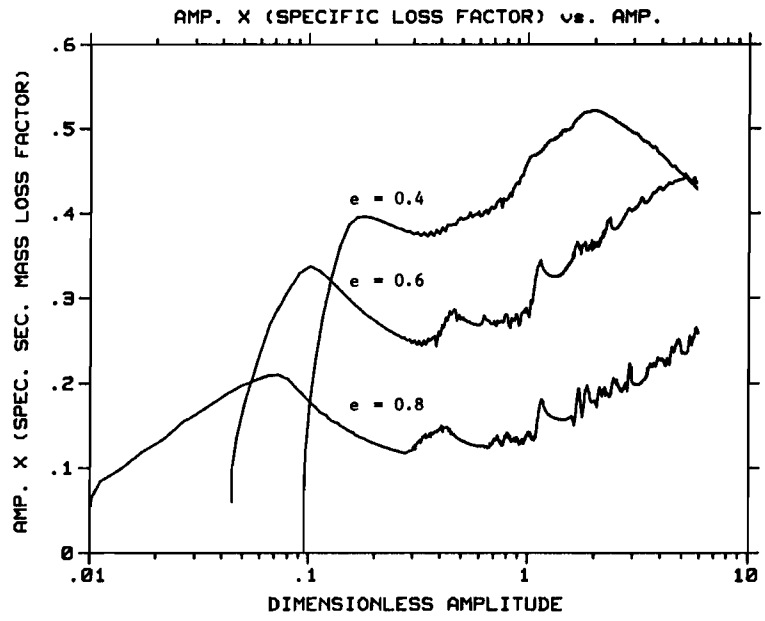

Figure 13 Amplitude Multiplied by Specific Secondary Mass Loss Factor for Three Values of the Coefficient of Restitution.
ν = 0.02; e = 0.4, 0.6, 0.

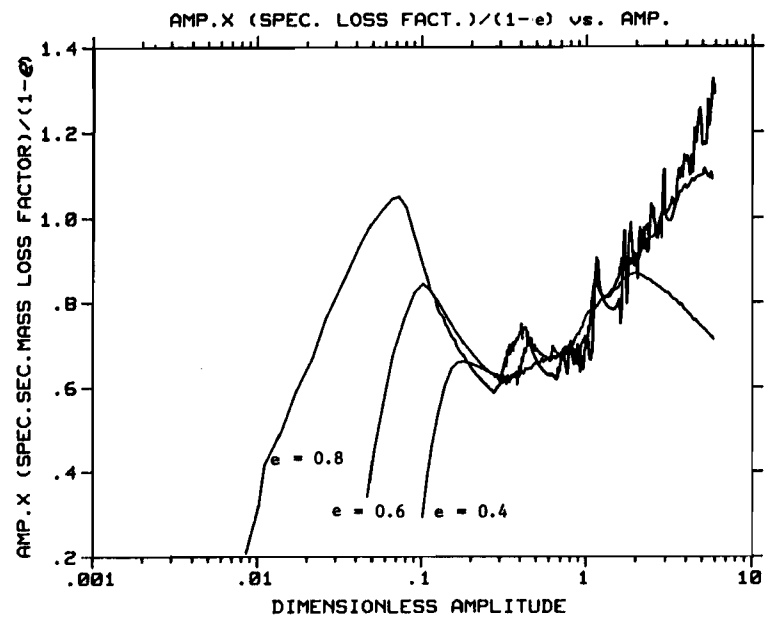

Figure 14 Amplitude Multiplied by the Specific Secondary Mass Loss Factor Divided by (1 - e) for Three Values of the Coefficient of Restitution. ν = 0.02; e = 0.4, 0.6, 0.8

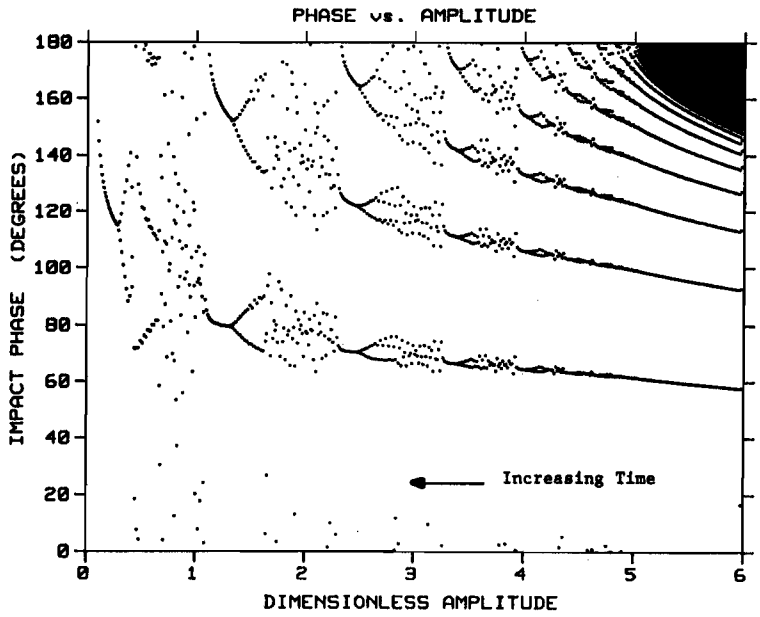

Figure 15 Impact Phase as a Function of Amplitude. $\nu = 0.02$; $e = 0.6$